

RESEARCH

Open Access



An approach based on P-wave velocity for grouting effectiveness evaluation in earthen sites

Weihao Li¹, Jingke Zhang^{1,2*}, Nan Wang¹, Yichen Zhang¹, Bojia Qi¹, Jiayi Chen¹ and Xingduo Yin¹

Abstract

Grouting technology is the primary method for repairing cracks in earthen sites. However, there has been a long-standing lack of effective methods for evaluating grouting effectiveness. This paper proposes a field evaluation method based on P-wave velocity. This method explicitly discusses two scenarios where the P-wave velocity of the grout is either higher or lower than that of the soil, using the depth h of the “hypothetical crack” as the evaluation indicator. The experimental results indicate that specimens with 20% and 40% defects show increases in h values of 0.0113 m and 0.0166 m, respectively. Laboratory tests have demonstrated that this method can accurately evaluate grouting effectiveness and is not affected by the P-wave velocity of the soil. The application of this evaluation method to three typical earthen sites resulted in more reliable and easily quantifiable evaluation outcomes. By considering the width of grout, the method provides a more intuitive comparison of reparation effectiveness. The study demonstrates the feasibility of the proposed method, thereby facilitating effective crack reparation in earthen sites.

Keywords Earthen sites, P-wave velocity, Non-destructive testing, Grouting, Effectiveness evaluation

Introduction

As important historical remnants and cultural symbols along the Silk Road, earthen sites hold significant historical, artistic, scientific, and cultural value [1]. These relics, constructed with earth as the main building material, have undergone severe deterioration over centuries of weathering [2]. Cracks, the most common form of deterioration observed on earthen sites, accelerate weathering and may lead to structural instability such as collapse [3]. Therefore, early reparation of cracks is imperative. Grouting technology is a commonly used reparation method in the field of civil engineering. By using chemical [4, 5]

or cementitious grouting [6, 7], cracks can be filled from within and sealed at the interface to prevent further deterioration of the structure.

The evaluation of grouting effectiveness has long plagued the development of crack reparation techniques. Due to the unique nature of cultural heritage conservation projects, any methods of detection that may cause damage are not permitted, significantly limiting the choice of equipment for effectiveness evaluation. Researchers have attempted to evaluate the grouting effectiveness through non-destructive testing methods such as ground-penetrating radar (GPR), thermal infrared imaging (TII), and P-wave velocity, but the results have been less than satisfactory. GPR has advantages in identifying significantly different substances or underground voids [8]. However, for the interior of repaired cracks, the differential signals of GPR are insufficient to accurately identify grout defects, thus failing to quantitatively evaluate grouting effectiveness. TII has been widely used in recent years, after reparation materials

*Correspondence:

Jingke Zhang
zhangjink@lzu.edu.cn

¹ School of Civil Engineering and Mechanics, Lanzhou University, Rd 222 Tianshui, Lanzhou, Gansu 730000, China

² Key Laboratory of Mechanics on Disaster and Environment in Western China of Ministry of Education, Lanzhou University, Lanzhou, Gansu 730000, China



© The Author(s) 2024. **Open Access** This article is licensed under a Creative Commons Attribution 4.0 International License, which permits use, sharing, adaptation, distribution and reproduction in any medium or format, as long as you give appropriate credit to the original author(s) and the source, provide a link to the Creative Commons licence, and indicate if changes were made. The images or other third party material in this article are included in the article's Creative Commons licence, unless indicated otherwise in a credit line to the material. If material is not included in the article's Creative Commons licence and your intended use is not permitted by statutory regulation or exceeds the permitted use, you will need to obtain permission directly from the copyright holder. To view a copy of this licence, visit <http://creativecommons.org/licenses/by/4.0/>. The Creative Commons Public Domain Dedication waiver (<http://creativecommons.org/publicdomain/zero/1.0/>) applies to the data made available in this article, unless otherwise stated in a credit line to the data.

are applied on the surface, distinct temperature differences are showed during changes in ambient temperature [9]. However, the results of TII are highly dependent on weather conditions, and inadequate understanding of various climatic factors can lead to errors in evaluation [10]. It has been generally confirmed that the velocity of P-waves is an important indicator of the integrity of rock and soil masses [11, 12]. Measuring the velocity of P-waves in rock and soil masses under different conditions is considered a useful technique for studying internal density changes and detecting defects [13]. Under the guidance of relevant acoustic wave propagation theories [14], researchers have explored the effects of the number, orientation, and aperture of cracks in rock and soil masses on the velocity of P-waves, thereby enhancing the understanding of the internal conditions. In the conservation of earthen sites, P-wave velocity has been employed to assess soil weathering degrees [15, 16] and examine the performance of modified grouts [17]. Experimental results have shown that there is a certain correlation between P-wave velocity and the mechanical strength parameters of the material [18, 19]. Additionally, P-wave velocity measurements have been directly applied to the detection of grouting and are considered a potential method for evaluating reparation effectiveness [20, 21].

In early studies, there were some unresolved issues associated with the use of P-wave velocity testing for assessing soil and rock masses, which constrained the application of this technique in evaluating the grouting effectiveness in earthen sites. Firstly, there existed an issue regarding travel distance error. It is generally believed that the velocity of homogeneous materials remains consistent and does not vary with changes in detection methods or measurement distances [22]. However, during actual detection processes, there is a phenomenon of abnormally increased wave velocity when the wave's travel distance is short [23], as depicted in Fig. 1. Due to the unknown of the specific propagation

path of the signal, the influence of this error is difficult to eliminate.

Nextly, there is the issue of soil non-homogeneity. As a naturally formed porous material, soil exhibits a complex and anisotropic internal structure [2]. Earthen sites where soil serves as the primary construction material have undergone hundreds of years of weathering, resulting in surface looseness and varying degrees of internal erosion [24]. Moreover, due to differential erosion phenomena, the physical data of the soil obtained from different locations are diverse [25]. Previously, in evaluating the grouting effect of cracks using P-wave velocity, a comparison was made between the wave velocity at intact structural locations and the measured locations [26]. Even with the averaging of wave velocity data from multiple locations, it remains scientifically unfeasible to select a single value that represents the local soil velocity. Addressing how to eliminate errors caused by soil non-homogeneity during detection and improving the reliability of local velocity measurements become crucial for evaluating the grouting effectiveness.

Lastly, there exists the issue of a lack of evaluation indicator. As mentioned above, the traditional method of evaluating effectiveness is based on comparing the velocity. The velocities at "intact" and repaired locations can only be relatively compared, incapable of providing a specific value as an evaluation criterion, thus limiting the widespread application of this evaluation method. In order to provide an intuitive expression of the grouting effectiveness, a new indicator needs to be proposed. Upon obtaining this indicator through evaluation methods and delineating a threshold range for it, the grouting effectiveness can be evaluated accordingly.

To enhance the reliability and applicability of grouting effectiveness evaluation, a field evaluation method based on P-wave velocity is proposed in this study. The general approach of this field evaluation method involves the hypothesis of one or two "cracks" to eliminate the wave velocity differential between the grout and the surrounding

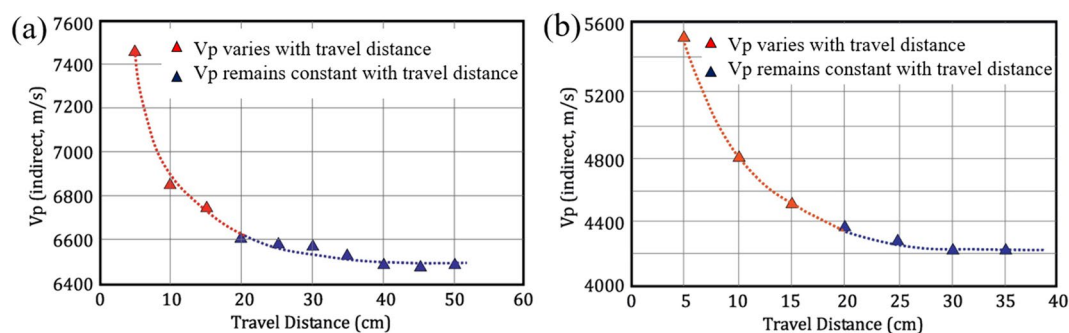


Fig. 1 Change in wave velocity depending on travel distance: **a** rock samples and **b** concrete samples [23]

soil after repair. The depth h of these “hypothetical cracks” is calculated and utilized as an indicator to evaluate the strength differences between the grout and the soil. The proposed method was effectively validated through laboratory model experiments in this study and was tested and evaluated at three typical earthen sites. The findings of this study offer valuable insights for improving grouting effectiveness evaluation techniques.

Methods

Crack depth estimation

The effectiveness of the repair is evaluated by detecting the decrease or increase in P-wave velocity, thereby determining the strength differences between the grout and the soil. Previously, this method has been used to estimate the depth of cracks in concrete. Unlike in concrete, where cracks only cause a decrease in overall P-wave velocity, grouted cracks can result in either an increase or decrease in P-wave velocity. These scenarios will be discussed in detail using Method A and Method B. First, the method for estimating crack depth in concrete based on P-wave velocity will be introduced, as the evaluation method in this study is an improvement based on the following research.

Due to the poor propagation capability of ultrasonic wave in air, the transmission time of waves increases significantly when there are defects in the medium [27]. Therefore, it is believed that ultrasonic waves bypass defects in the medium. Based on this assumption, Bungey [28] proposed a mathematical expression for estimating the crack penetration depth “ h ” by comparing the time-of-flight of an ultrasonic wave through sound concrete (T_S) to that around a crack (T_C). Measurements of time-of-flight values at sound concrete (T_S) need to be conducted additionally. Considering the wave travel path depicted in Fig. 2a, the crack depth h can be calculated by Eq. (1).

$$h = \left(\frac{x}{T_S} \right) \sqrt{T_C^2 - T_S^2} \tag{1}$$

where x is the distance from a single transducer to the crack.

Bungey’s method exhibits notable similarities with current approaches for evaluating grouting effectiveness in earthen sites. The non-homogeneity of soil renders comparison P-wave velocity with intact soil unreliable. The assumption of the same ultrasonic pulse velocity through a sound concrete and through a path around the crack may introduce inaccuracies in crack depth estimations. According to Bungey, the estimation precision for the depth of cracks using Eq. (1) is approximately 15%.

The method proposed by the British Standard BS 1881: Part 203 [29] eliminates the need for additional measurement of sound concrete (Fig. 2b). It involves obtaining data from two sets of transducers positioned at distances x and $2x$ from the crack, respectively, and calculating the crack depth h by Eq. (2).

$$h = x \sqrt{\frac{4T_1^2 - T_2^2}{T_2^2 - T_1^2}} \tag{2}$$

where T_1 and T_2 are the time-of-flight of the wave with transducers at distances x , and $2x$ from the crack, respectively.

Pinto [30] improved BS 1881’s method, resulting in Eq. (3), wherein a linear relationship between x_i^2 and $(T_i - T_i/2)^2$ was identified. Data processing was conducted through graphical methods to obtain the crack depth h . As illustrated in Fig. 2c, the first position should have both transducers equidistantly from the crack while for the other ones the receiver is moved in fixed increments. While this method exhibits some applicability, particularly for cracks near the edges of structures, it is less suitable for earthen sites where the majority of cracks are closely spaced.

$$h = \sqrt{V^2 \left(T_i - \frac{T_1}{2} \right)^2 - x_i^2} \tag{3}$$

where T_i is the time-of-flight measured with transducers at a distance x_i from the crack; V is the ultrasonic pulse velocity.

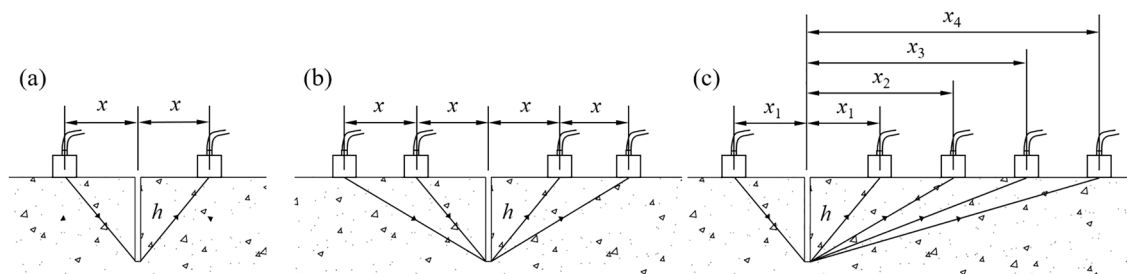


Fig. 2 Transducer arrangements for **a** Bungey’s, **b** BS 1881 and **c** Pinto’s methods

Method A

Due to the variations in reparation materials and the properties of soils, two scenarios may arise where the soil velocity is either higher or lower than that of the reparation material. Correspondingly, two methods, Method A and Method B, have been proposed to evaluate the grouting effectiveness. Method A is applicable when the wave velocity of the grout is lower than that of the soil after reparation.

When a crack is filled with grout, the process is not perfect. Due to decreasing injection pressure away from the injection point, grout may not reach every corner of the crack, resulting in voids in localized areas. Simultaneously, the flowing grout rapidly shrinks due to water loss, leading to certain small cracks that diminish the quality of grouting. To assess the quality of this reparation with a measurable indicator rather than relying on difficult-to-measure parameters such as void volume, number of shrinkage cracks, length, and width, this method proposes substituting all grouting defects with a “hypothetical crack”. As shown in Fig. 3, all reductions in wave velocity due to grouting defects can be equivalently represented as wave transmission passing through this “hypothetical crack”. Figure 3a depicts the actual scenario where signals propagate from one transducer, through the soil, encountering grout with defects whose specific extent is unknown, and finally through the soil to another transducer. Figure 3b illustrates the assumption made by Method A, where defects in the grout are replaced by a “hypothetical crack”. Because ultrasonic signals must “travel around” this hypothetical crack, transmission time increases. The increased transmission distance in Fig. 3b is equivalent to the wave velocity reduction caused by grouting defects in Fig. 3a, thus allowing the depth h of the hypothetical crack to reflect the extent of grouting defects. Under this circumstance, the v corresponds to the P-wave velocity of the soil along the measurement line, while the depth h of the crack reflects the difference in velocities between the grout and the soil. By simultaneously adjusting the distance between two transducers to maintain the crack centrally positioned, thus

minimizing interference from adjacent cracks. For ease of application, the distance between two transducers is denoted as x_i , resulting in Eq. (4):

$$\left(\frac{v}{2}T_i\right)^2 = \left(\frac{1}{2}x_i\right)^2 + h^2 \tag{4}$$

through simplification, it can be shown in Eq. (5):

$$T_i^2 = \frac{1}{v^2}x_i^2 + \frac{4}{v^2}h^2 \tag{5}$$

where T_i is the time-of-flight measured with transducers at a distance of x_i from each other.

Therefore, a linear correlation between x_i^2 and T_i^2 is obtained, and data processing can be conducted through graphical methods to determine the crack depth h and the P-wave velocity v .

Method B

When the P-wave velocity of the grout is higher than the soil, the situation becomes slightly more complex, and hypothesis as one single crack is no longer feasible. This phenomenon is frequently observed in the earthen sites due to the weathering effects, resulting in the friable and loose of the soil. Consequently, there is a decrease in density of the soil, particularly on the surface of the earthen site. Under such circumstances, the Eq. (5) mentioned in Sect. “Method A” is inapplicable. Modifications are needed to derive an indicator that can reflect the evaluation. As shown in Fig. 4, the soil should be considered as the grout with cracks. The purpose is to eliminate the difference in P-wave velocities between the soil and grout, and the added cracks increase the propagation distance of the waves. Notably, the width of the grout w cannot be disregarded, as the crack depth h is significantly influenced by w . The calculation equation can be expressed as:

$$(x_i - w)^2 + 4h^2 = (vT_i - w)^2 \tag{6}$$

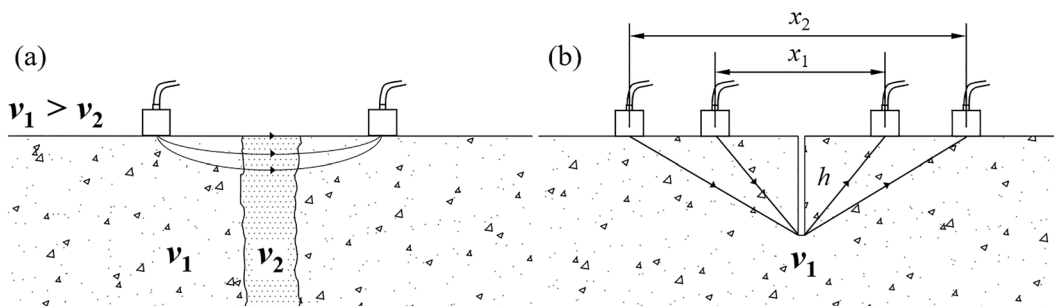


Fig. 3 Transducer arrangements for method A under **a** actual conditions and **b** hypothetical conditions

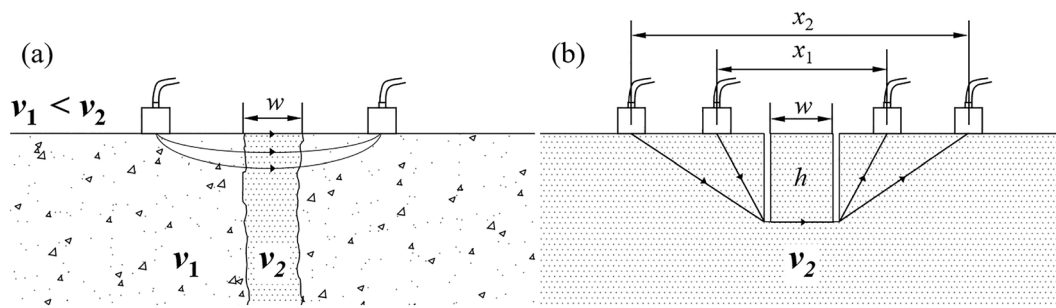


Fig. 4 Transducer arrangements for method B under **a** actual conditions and **b** hypothetical conditions

where T_i is the time-of-flight measured with transducers at a distance of x_i from each other, v is the P-wave velocity of the grout.

With two sets of x_i and T_i , the equation can be solved using MATLAB to get a unique positive solution. h now reflects the degree that P-wave velocity of the grout exceeding the soil. However, the strength of the grout should be close to or slightly higher than that of the soil. Excessive strength of the grout destroys the consistency of the earthen sites, which is also considered improper conservation. Therefore, a smaller h is considered to meet the requirements.

Data collection and processing

Upon obtaining a set of data from detection, an initial assumption can be made that the wave velocity of the repair material is lower than that of the soil. Method A can be applied, and the solution can be derived using graphical methods. Two scenarios may arise: one in which h^2 is greater than zero, allowing for the calculation of h ; and one in which h^2 is less than zero, which is clearly incorrect. Thus, the initial assumption is erroneous, and the wave velocity of the repair material is higher than that of the soil. Consequently, Method B should be used to solve the problem, yielding a unique positive solution.

Regardless of whether methods are applied, two sets of independent data are enough to meet the requirements. However, for reliability in calculations, it is necessary to provide clarification regarding the selection of data. The first set of measuring data is collected starting from a travel distance of 5 cm, followed by horizontal movement of the transducers at intervals of 10 cm, 15 cm, 20 cm, and so forth, until data cannot be obtained. Due to insufficient P-wave propagation energy, measurements are typically limited to distances of 25–40 cm, which depends on the instrument model and the properties of the soil. Additionally, data with travel distance less than the width of the grout are not required to be measured. The evaluation results are plotted according to Eq. (5) and shown in Fig. 5. It can be observed that data with spacing

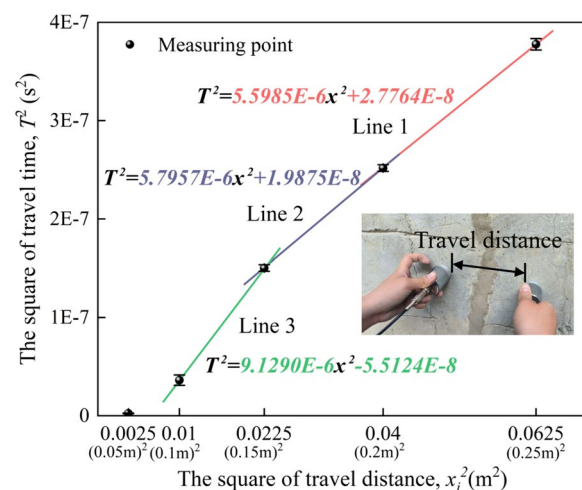


Fig. 5 Measuring points and fitting lines according to method A

Table 1 Relevant parameters of fitting lines

Fitting line	Slope ($\frac{1}{v^2}$)	Intercept ($\frac{4}{v^2} h^2$)	h (m)	V (m/s)
1	9.1290E-6	- 5.5124E-8	/	330.9698
2	5.7957E-6	1.9875E-8	0.0586	415.3814
3	5.5985E-6	2.7764E-8	0.0704	422.6337

over 15 cm are relatively stable and exhibit a linear correlation, while data within 15 cm are more scattered. Since the lack of clarity regarding the exact propagation pattern of signals, the challenge persists in mitigating P-wave velocity errors attributed to travel distance. It is currently acknowledged that narrow distance between transducers can influence P-wave velocity, with this influence escalating exponentially as distance diminishes. Referencing Ersoy’s research [23], it is noted that the distance exceeding 20 cm between transducers minimizes their influence on P-wave velocity. Table 1 presents the relevant parameters of different data. It can be inferred that data with larger travel distance are closer and more accurate. When

selecting data for calculation, priority should be given to using the two sets of data with the maximum travel distance. In cases where there are three or more sets of stable data, results can also be obtained by considering pairwise combinations of the data and taking the average value.

Laboratory testing

To verify the reliability of the aforementioned method in practical detection, a laboratory model experiment was designed to simulate cracks in earthen sites and conduct grouting reparations. Due to the theoretical consistency between Method A and Method B, only Method A was validated in this laboratory experiment.

Materials

The experimental soil was sourced from the collapsed site of the Ming Great Wall in Gaotai County, Gansu Province, China. The reinforcement material chosen was traditional Chinese hydraulic lime, Calcined Ginger Nut (CGN), which has been proven effective for repairing cracks in earthen sites [31]. Table 2 presents the basic physical properties of the soil, while Table 3 shows the XRD results for CGN.

Specimen preparation

To simulate field testing conditions and accommodate the experimental timeline, square soil specimens measuring 30×15×15 cm were prepared. A space of 4×6×10 cm was left on the top surface of each specimen to simulate cracks (Fig. 6). The sampling process involved: (1) crushing the soil and sieving it through a 1 mm sieve; (2) based on compaction test results, adding distilled water to the soil and sealing it for over 24 h to reach optimum moisture content; (3) pouring the moist soil into molds and compacting it in layers, inserting stainless steel wedges to create spaces for simulating cracks, and removing the wedges after molding; (5) naturally curing the samples in laboratory conditions (T: 25 ± 5 °C, RH: 20 ± 5%) until achieving stable quality.

Table 2 Physical properties of soil

Property	Unit	Value
Natural moisture content	%	1.72
Natural density	g/cm ³	1.65
Specific gravity		2.47
Maximum dry density	g/cm ³	1.59
Optimum moisture content	%	41.55
Coefficient of non-uniformity		10.0
Coefficient of curvature		1.60

Table 3 Semiquantitative analysis result of CGN by XRD

Formula	By mass/%
CaO	27.4
SiO ₂	22.3
Ca(OH) ₂	7.0
β-CaSiO ₃	28.7
Ca ₂ Al ₂ Si ₂ O ₈	14.6

The reparation material consisted of a slurry with a mass ratio of CGN to site soil of 1:10 and a water-cement ratio of 0.45 [32]. An electric grout mixer (280 rpm, 120 s) was utilized for preparing the grout. To artificially control the quality of grouting, plastic bubbles of specific volumes were used as defects in the grout. During grouting, these plastic bubbles were uniformly dispersed into the cracks. The volumes of plastic bubbles occupied 0%, 20%, and 40% of the crack volume, respectively, to simulate varying degrees of defects.

P-wave velocity test

After stabilizing the specimen's mass post-grouting, P-wave velocity testing was conducted. Transducers were positioned on either side of the cracks at intervals of 10 cm, 15 cm, 20 cm, and 25 cm (Fig. 7). Travel times of the signal were recorded at different intervals and data were organized accordingly. As shown in Fig. 8, a noticeable increase in wave velocity anomalies occurred at a 10 cm transducer distance, with slight anomalies observed at 15 cm. Following the guidelines in Sect. "Data collection and processing" for data selection, data from transducer distances of 20 cm and 25 cm were chosen for analysis in this laboratory experiment. Furthermore, it was observed that with increased defect severity, the travel times at the same intervals gradually increased while the wave velocity decreased, demonstrating that

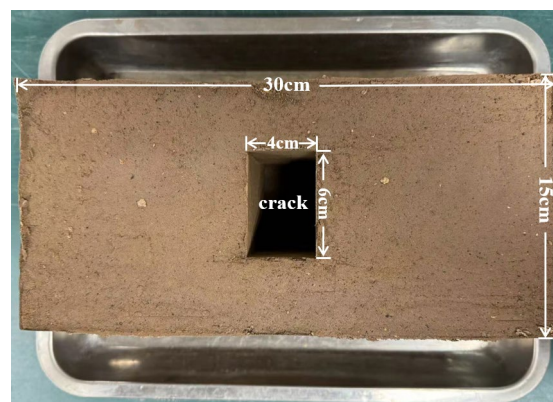


Fig. 6 The model for laboratory test

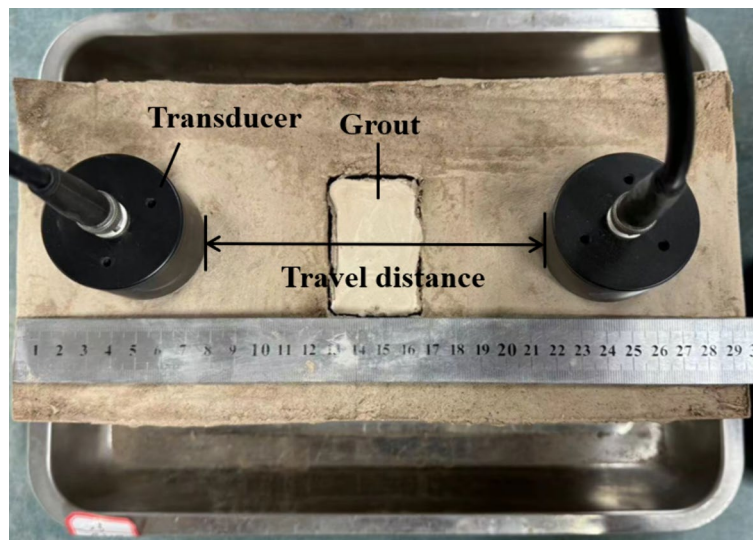


Fig. 7 P-wave velocity test

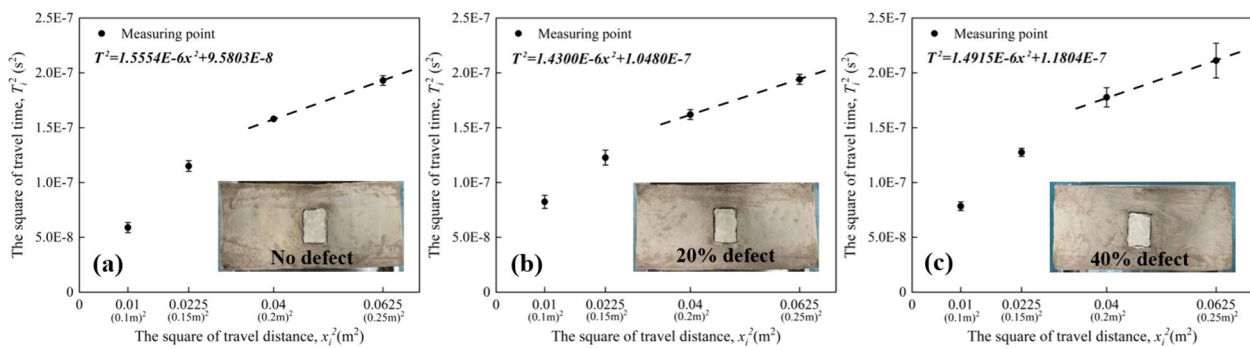


Fig. 8 Measuring points of specimens with **a** no defect, **b** 20% defect and **c** 40% defect according to method A

Table 4 Relevant parameters of specimens

Defect%	Mass of grout/g	Slope ($\frac{1}{v^2}$)	Intercept ($\frac{4}{v^2} h^2$)	h (m)	V (m/s)
0	486	1.5554E-6	9.5803E-8	0.1241	801.8238
20	403	1.4300E-6	1.0480E-7	0.1354	836.2420
40	318	1.4915E-6	1.1804E-8	0.1407	818.8199

the addition of plastic bubbles can degrade grouting effectiveness and detect differences.

Using method A, evaluations were conducted on three groups of specimens, and the results are summarized in Table 4. In addition to basic parameters, Table 4 also records the grout mass during injection: for grout with 20% defects, the mass was approximately 82.92% compared to no defect grout, and for grout with 40% defects, the mass was approximately 65.43%, which

closely approximates the design values. The variations in h values align with experimental expectations; specimens with 20% and 40% defects showed increases in h values of 0.0113 and 0.0166, respectively, compared to no defect specimens. The increasing trend in h values across the three groups demonstrates the effectiveness of this method.

Furthermore, due to inherent specimen variations, their wave velocity values were not identical. Specimen with 20% defects exhibited higher wave velocities in the soil portion compared to no defect specimens. Even so, the h values of specimens with 20% defects remained higher than those of no defect samples, demonstrating the method's effectiveness in evaluating grouting outcomes and its ability to mitigate the influence of surrounding soil wave velocities. Unfortunately, the h values across the three groups did not differ by 20% or more as anticipated. This discrepancy is due to the laboratory experiments where the specimens were fresh and dense,

resulting in wave velocity values nearly double those observed at field sites. Despite this, the grout used was almost identical to that used in the field. Consequently, after field grouting, the wave velocities of the repair materials approached those of the soil, whereas they differed significantly in laboratory experiments. The h values from this test results consistently remained at higher levels.

Field application and discussion

Test site descriptions

Three typical earthen sites were selected for the application of grouting effectiveness evaluation. Jinsha site was discovered in Chengdu City, Sichuan Province. The Relics Hall has been constructed at the excavation site by the Jinsha Site Museum for the protection, study, and exhibition of Jinsha culture and ancient Shu civilization. The cracks were grouted for reparation in 2012, but the specific reparation measures were not formally documented. As shown in Fig. 9, the grouted cracks are distributed on the walls, floors, and aisles formed during the excavation of the sacrificial area. P-wave velocity tests are conducted on these grouted cracks to investigate whether different locations have an impact on the grouting effectiveness.

The Suoyang Ancient City is located in Suoyangcheng Town, Guazhou County, Gansu Province. It is a world-famous earthen heritage site along the ancient Silk Road, which represents one of the largest and most

well-conserved ancient Han and Tang dynasty cities in the northwest region of China. The continuous weathering over the years has led to severe deterioration of the walls, resulting in numerous cracks. In 2022, a grouting reparation was conducted on some of the walls by the Dunhuang Academy, preceded by grouting experiments on a test wall to ensure the effectiveness of the reparation measures. The effectiveness evaluation selected grouted cracks on the test wall, part of the inner city east wall, and part of the Ta'er Temple wall, as shown in Fig. 9.

Qiaowan Ancient City is located in Guazhou County, Gansu Province. It was initially constructed during the Qing Dynasty and was declared a provincial-level cultural relic protection unit in 2016. Due to natural environmental influences, the wall of the Qiaowan Ancient City has developed numerous cracks. In 2021, the Dunhuang Academy conducted grouting reparation on the cracks. Detailed information about the selected earthen sites presented in Table 5. The detection employed the ZT801 nonmetal ultrasonic apparatus (Zhongtuo Tech, China) at a frequency of 100 kHz.

Results

Due to the lower wave velocity of the grout compared to that of the soil in Jinsha site, method A is employed for evaluation. The tests are conducted on 106 representative grouted cracks, with the results shown in Table 6. The evaluation indicator h ranges from a minimum of

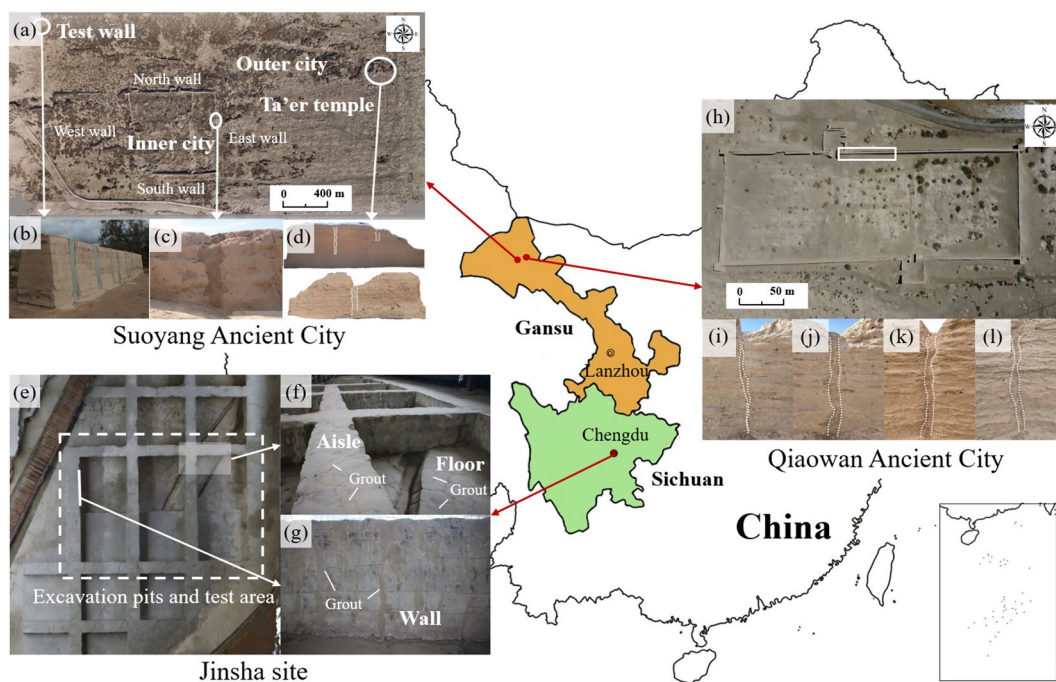


Fig. 9 Distribution of selected earthen sites: **a–d** Suoyang Ancient city, **e–g** Jinsha site, **h–l** Qiaowan Ancient city

Table 5 Detailed information about the selected earthen sites

Earthen site	Environment	Soil moisture/%	Crack's location	Evaluation method	Reparation material
Jinsha site	Arid	4.76 [33]	Wall Aisle Floor	Method A	Unknown
Suoyang Ancient City	Arid	0.5–1.5 [34]	Test wall Wall	Method A Method A & B	Collapsed site soil mixed with hydraulic lime
Qiaowan Ancient City	Humid	0.93 [35]	Wall	Method B	Collapsed site soil mixed with hydraulic lime

Table 6 P-wave velocities obtained from the wall, floor and aisle of Jinsha site

Location	Wall	Floor	Aisle
Maximum h (m)	0.0876	0.0788	0.0757
Minimum h (m)	0.0011	0.0046	0.0048
Average h (m)	0.0275	0.0299	0.0277
Maximum v (m/s)	421.10	410.33	408.67
Minimum v (m/s)	295.41	299.56	306.94
Average v (m/s)	336.51	339.61	340.94

0.0011 m to a maximum of 0.0876 m, all of which did not exceed 0.1 m. The wave velocities ranges from 295.41 m/s to 421.10 m/s. Overall, there are no significant differences in the grouting effectiveness at different locations, but both the maximum value of *h* and the wave velocity are observed on the walls. Figure 10a illustrates the relationship between *h* and *v*. It can be observed from the graph that the values of *h* mainly concentrated in the range of 0.01–0.04 m, while *v* concentrated in the range of 320 m/s to 360 m/s. There is a positive correlation

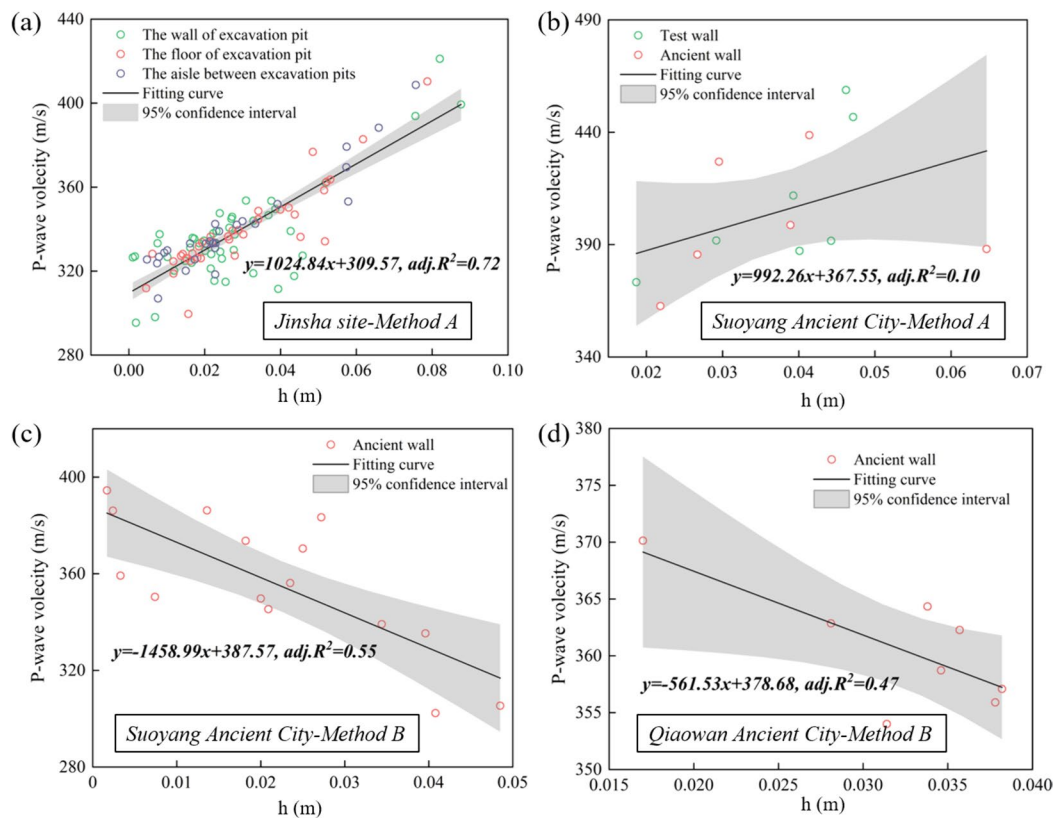


Fig. 10 Change in P-wave velocity depending on *h* of **a** Jinsha site, **b** and **c** Suoyang Ancient City, **d** Qiaowan Ancient City

between h and v , with the adjusted r-squared value being 0.72.

Unlike the Jinsha site, the Suoyang Ancient City and Qiaowan Ancient City are entirely exposed to outdoor environments. The harsh natural conditions in the northwest region of China, such as strong winds carrying sand and occasional heavy rainfall, have led to poor conservation conditions. Consequently, there is a phenomenon where the wave velocity of the grout exceeds that of the soil. However, this phenomenon is not observed on the artificially rammed test walls, where the overall wave velocity is slightly higher than that of the ancient walls.

In Suoyang Ancient City, the wave velocity of the grout on the test walls and some of the cracks on the ancient walls is lower than that of the soil, hence method A is applied for evaluation. For the other cracks, where the wave velocity of the grout is higher than that of the soil, method B is used for evaluation, with results present in Fig. 10b and c, respectively. When the wave velocity of the grout is lower than that of the soil, the indicator h shows a positive correlation with the wave velocity. However, the adjusted r-squared value is only 0.1, much lower than the test results at the Jinsha site. This could be attributed to the higher surface roughness of the Suoyang Ancient City walls compared to those at the Jinsha site, as surface roughness alters the propagation path of waves on the surface. When the wave velocity of grout is higher than that of the soil, the indicator h shows a negative correlation with the wave velocity, with an adjusted r-squared value of 0.55. Besides, h , calculated by method B, is lower than the results calculated by method A. Nevertheless, comparing h obtained from the two methods is meaningless due to their differences in quantity and implication.

Previous studies applied P-wave velocity tests on several grouted cracks in Qiaowan Ancient City [35]. Upon reanalyzing the data, it is found that the P-wave velocity of the grout is consistently higher than that of the soil. Therefore, method B is utilized to calculate h , with results illustrated in Fig. 10d. The indicator h ranges from a minimum of 0.017 cm to a maximum of 0.038 cm, with the majority exceeding 0.03 cm. Wave velocities are concentrated between 350 m/s and 370 m/s. The wave velocities closely match those of the Suoyang Ancient City’s soil (evaluated by method B), but the average h is approximately 47% higher than that of Suoyang Ancient City. A higher h indicates denser grout compared to the surrounding soil. The indicator h shows a negative correlation with wave velocity, with an adjusted r-squared of 0.47.

Early evaluation results indicate that wave velocity of most grouted cracks at the Qiaowan Ancient City is higher than the surrounding soil, with a small portion

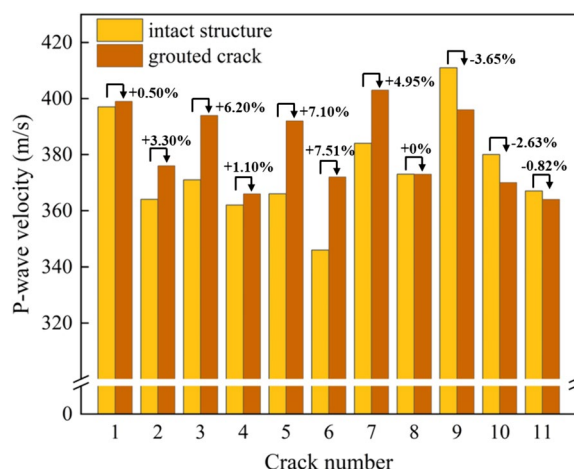


Fig. 11 Grouting effectiveness evaluation of Qiaowan Ancient city with former method

exhibiting lower velocities (Fig. 11). Upon reevaluation, it is found that all of the grouted cracks had higher wave velocities than the soil. Hence, it can be inferred that the early evaluation methods had certain limitations. The data obtained by comparing the wave velocities of the grouted cracks with those of “intact” soil nearby are not accurate. Moreover, the early evaluation methods cannot directly compare the measured results, only indicating how much the wave velocity of the grouted cracks has increased or decreased compared to the “intact” soil. The introduction of the indicator h offers the potential for quantitatively evaluating the grouting effectiveness of earthen site cracks. Additionally, the experimental results indicate that there is no correlation between soil moisture content and P-wave velocity. For the same type of soil, moisture content can affect the P-wave velocity [36]. For different earthen sites, the composition and physical properties of the soil vary significantly, and P-wave velocity is influenced by multiple factors. This phenomenon also indirectly suggests that earthen site assessments should reference the specific site itself, making it difficult to provide a certain value for evaluating different sites across various regions and environments.

Analysis with grout width

In previous evaluations of the grouting effectiveness of cracks, little consideration has been given to the influence of grout width. However, the width of grout, as a representation of crack width and volume after grouting, should be taken into account. The relationship between grout width w and h is depicted in Fig. 12, with separate analyses conducted due to the differing implications of h derived from method A and B.

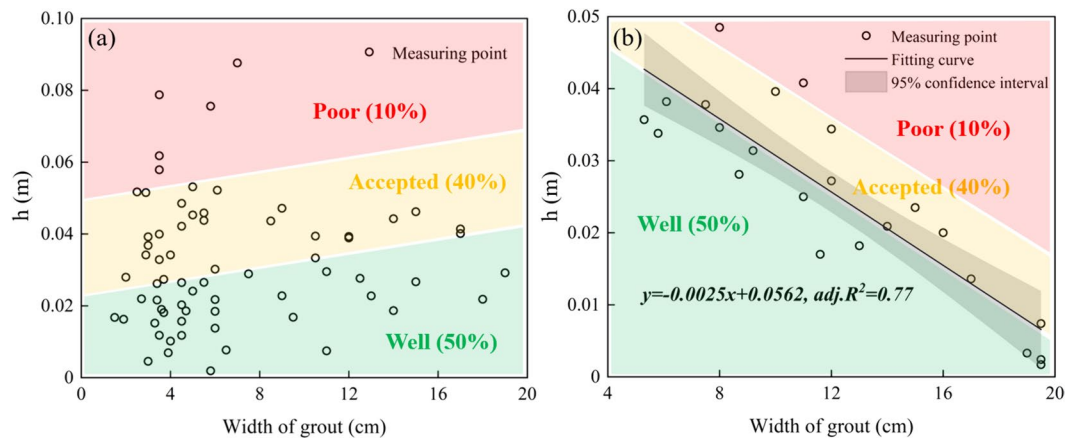


Fig. 12 Change in h depending on width of grout: **a** method A, and **b** method B

In Eq. (5) of method A, h is a quantity independent of the grout width, as the results shown in Fig. 12a. The grout width, can be regarded as an independent variable in the evaluation. Irregularities in cracks lead to uncertain defects during grouting construction, with the general consensus being that these construction defects become more pronounced with larger crack width. Therefore, when the obtained h values are the same, the grouting effectiveness with wider grout is superior to that with narrower ones. Due to the lack of scientifically defined thresholds, the grouting effectiveness of each crack cannot be definitively determined. It is assumed that that 50% of the grouted cracks exhibit good grouting effectiveness, 40% exhibit accepted grouting effectiveness, and 10% exhibit poor grouting effectiveness, enabling a relative delineation of evaluation results for reference.

In Eq. (6) of method B, h is influenced by the grout width. As illustrated in Fig. 12b, there is a negative correlation between the grout width and h , with an adjusted R-squared of 0.77. Assuming constant velocity of grout, soil, and detection distance (v and x_i remain constant), as the grout width increases (w increases), the required time-of-flight will decrease (T_i decreases). Rewriting Eq. (6) as Eq. (7) reveals that both terms multiplied on the right side decrease, thus h decreases. Furthermore, as the grout width w approaches the distance of transducers x_p , h approaches 0. Additionally, it is possible that the increase in grout width leads to grouting defects, causing the velocity of the grout to decrease.

$$4h^2 = (vT_i + x_i - 2w) \cdot (vT_i - x_i) \tag{7}$$

When the grout width exceeds 18 cm, h is less than 0.01 m. However, due to the absence of cracks with wider grout widths and the limited detection length of the instrument, it is currently unclear whether the velocity of

the grout would be lower than that of the soil with continued increases in grout width. Similarly, the evaluation results are relatively categorized as good, accepted, or poor and displayed in different colors.

Conclusions

A field evaluation method for grouting in earthen sites based on P-wave velocity is provided in this study. Two scenarios, differing in grout and soil wave velocities, are discussed, using the depth h of a “hypothetical crack” as the evaluation indicator. Laboratory experiments were designed to verify the reliability of this method, and field tests were conducted at three earthen sites. Based on the results, the following conclusions can be drawn:

- (1) The use of the proposed method to evaluate the effectiveness of grouting is feasible. Compared to traditional evaluation methods, this approach does not require a comparison with the velocity at “intact structure”, thus enhancing detection reliability. The introduction of the quantitative indicator h renders the detection results more scientific and reasonable.
- (2) Laboratory test results indicate that when grouting defects are 20% and 40%, the h values increase by 0.0113 m and 0.0166 m, respectively. This demonstrates that the method can accurately evaluate the repair effectiveness and is not affected by the local soil wave velocity.
- (3) The recalculated velocity data of the Qiaowan Ancient City, which eliminates errors caused by the non-homogeneous of the wall, has yielded more accurate evaluation results. A comparison between the proposed and traditional evaluation methods can provide insights for further development in effectiveness evaluation.

- (4) The depth of the hypothetical crack h , combined with the grout width, enables an effective evaluation of grouted cracks. However, due to the limited amount of data, there is a lack of scientifically defined thresholds to categorize the effectiveness. In the future, through extensive indoor and field experiments, the criteria for both evaluation methods can be determined separately to facilitate engineering detection.

Acknowledgements

The authors would like to thank Dunhuang Academy for the valuable help in the investigation. We also thank the editors and reviewers for their time dedicated to evaluating our work.

Author contributions

WL: (1) Conceptualization; (2) Methodology; (3) Writing and Editing; JZ: (1) Writing and Revision; (2) Project Leadership and Conceptualization; (3) Funding acquisition; NW: (1) Conceptualization; (2) Methodology; YZ and BQ: and Investigation. JC and XY: Data Curation. All authors have read and approved the final manuscript.

Funding

The work is funded by the Fundamental Research Funds for the Central Universities (Izuibky-2024-it18) and the Major Special Project of Science and Technology in Gansu Province (Grant No. 23YFFA0008).

Data availability

All data sources have been listed in the manuscript. The datasets used and analyzed during the current study are available from the corresponding author upon reasonable request.

Declarations

Competing interests

The authors declare no competing interests.

Received: 15 April 2024 Accepted: 8 August 2024

Published online: 14 August 2024

References

- Li L, Shao M, Wang S, Li Z. Preservation of earthen heritage sites on the Silk Road, northwest China from the impact of the environment. *Environ Earth Sci*. 2011;64:1625–39. <https://doi.org/10.1007/s12665-010-0829-3>.
- Miccoli L, Müller U, Fontana P. Mechanical behaviour of earthen materials: a comparison between earth block masonry, rammed earth and cob. *Constr Build Mater*. 2014;61:327–39. <https://doi.org/10.1016/j.conbuildmat.2014.03.009>.
- Li Z, Wang X, Sun M, Chen W, Guo Q, Zhang H. Conservation of Jiaohe ancient earthen site in China. *J Rock Mech Geotech*. 2011;3:270–81. <https://doi.org/10.3724/SP.J.1235.2011.00270>.
- Sui W, Liu J, Hu W, Qi J, Zhan K. Experimental investigation on sealing efficiency of chemical grouting in rock fracture with flowing water. *Tunn Undergr Space Technol*. 2015;50:239–49. <https://doi.org/10.1016/j.tust.2015.07.012>.
- Müller U, Miccoli L, Fontana P. Development of a lime based grout for cracks repair in earthen constructions. *Constr Build Mater*. 2016;110:323–32. <https://doi.org/10.1016/j.conbuildmat.2016.02.030>.
- Yang Y, Chen B, Chen Y, Liu F, Xie X, Guo W, Wang H. Effect of admixtures and PVA fiber on the mechanical properties of high strength cementitious grout. *Case Stud Constr Mat*. 2023;18:e01884. <https://doi.org/10.1016/j.cscm.2023.e01884>.
- Yang Y, Chen B, Chen Y, Liu F, Xie X, Guo W, Wang H. Development of a high strength cementitious grout for filling the joints of UHPC permanent formwork. *Dev Built Environ*. 2023;13:100120. <https://doi.org/10.1016/j.dibe.2023.100120>.
- Zhang F, Xie X, Huang H. Application of ground penetrating radar in grouting evaluation for shield tunnel construction. *Tunn Undergr Sp Tech*. 2010;25:99–107. <https://doi.org/10.1016/j.tust.2009.09.006>.
- Cui K, Feng F, Chen W, Wang D, Wang X. Slurry and technology optimization for grouting fissures in Earthen Sites with quicklime. *Adv Mater Sci Eng*. 2019;2019:1–11. <https://doi.org/10.1155/2019/9076760>.
- Lehmann B, Ghazi Wakili K, Frank T, Vera Collado B, Tanner C. Effects of individual climatic parameters on the infrared thermography of buildings. *Appl Energ*. 2013;110:29–43. <https://doi.org/10.1016/j.apenergy.2013.03.066>.
- Shi S, Li S, Li L, Zhou Z, Wang J. Advance optimized classification and application of surrounding rock based on fuzzy analytic hierarchy process and tunnel seismic prediction. *Automat Constr*. 2014;37:217–22. <https://doi.org/10.1016/j.autcon.2013.08.019>.
- Zhang J, Li Z, Li L, Liu J, Liu D, Shao M. Study on weathering mechanism of sandstone statues in Southwest China: example from the sandstone of Niche of Sakyamuni entering Nirvana at Dazu Rock Carvings. *Nat Hazards*. 2021;108:775–97. <https://doi.org/10.1007/s11069-021-04705-w>.
- Fais S, Casula G. Application of acoustic techniques in the evaluation of heterogeneous building materials. *NDT E Int*. 2010;43:62–9. <https://doi.org/10.1016/j.ndteint.2009.10.004>.
- Shen H, Li X, Li Q, Wang H. A method to model the effect of pre-existing cracks on P-wave velocity in rocks. *J Rock Mech Geotech Eng*. 2020;12:493–506. <https://doi.org/10.1016/j.jrmge.2019.10.001>.
- Wang X, Guo Q, Yang S, Zhang D, Wang Y. Nondestructive testing and assessment of consolidation effects of earthen sites. *J Rock Mech Geotech*. 2016;8:726–33. <https://doi.org/10.1016/j.jrmge.2016.06.001>.
- Richards J, Guo Q, Viles H, Wang Y, Zhang B, Zhang H. Moisture content and material density affects severity of frost damage in earthen heritage. *Sci Total Environ*. 2022;819:153047. <https://doi.org/10.1016/j.scitotenv.2022.153047>.
- Zhang L, Zhang J, Wen X, Li W, Zhao L. Durability assessment of calcined ginger nuts-based anchor grouts used in the conservation of Earthen sites. *Int J Archit Herit*. 2023;17:1388–403. <https://doi.org/10.1080/15583058.2022.2038306>.
- Yagiz S. P-wave velocity test for assessment of geotechnical properties of some rock materials. *Bull Mater Sci*. 2011;34:947–53. <https://doi.org/10.1007/s12034-011-0220-3>.
- Galán-Marín C, Rivera-Gómez C, Bradley F. Ultrasonic, molecular and mechanical testing diagnostics in natural fibre reinforced, polymer-stabilized earth blocks. *Int J Polym Sci*. 2013;2013:130582. <https://doi.org/10.1155/2013/130582>.
- Shiotani T, Momoki S, Chai H, Aggelis DG. Elastic wave validation of large concrete structures repaired by means of cement grouting. *Constr Build Mat*. 2009;23:2647–52. <https://doi.org/10.1016/j.conbuildmat.2009.01.005>.
- Aggelis DG, Hadjiyiannou S, Chai HK, Momoki S, Shiotani T. Longitudinal waves for evaluation of large concrete blocks after repair. *NDT E Int*. 2011;44:61–6. <https://doi.org/10.1016/j.ndteint.2010.09.007>.
- Rodríguez P, Celestino TB. Assessment of damage distribution in brittle materials by application of an improved algorithm for three-dimensional localization of acoustic emission sources with P-wave velocity calculation. *Constr Build Mater*. 2020;231:117086. <https://doi.org/10.1016/j.conbuildmat.2019.117086>.
- Ersoy H, Karahan M, Babacan AE, Sünnetci MO. A new approach to the effect of sample dimensions and measurement techniques on ultrasonic wave velocity. *Eng Geol*. 2019;251:63–70. <https://doi.org/10.1016/j.enggeo.2019.02.011>.
- Zhang Y. Knowledge of earthen heritage deterioration in dry areas of China: salinity effect on the formation of cracked surface crust. *Herit Sci*. 2023;11:41. <https://doi.org/10.1186/s40494-023-00890-y>.
- Guo Z, Qi Q, Zhang S, Chen W, Wu C, Wu H. Study on the characterization of differential weathering feature based on surface roughness theory and 3D laser scanning: a case study of the Suoyang Ancient City. *J Cult Herit*. 2023;62:449–59. <https://doi.org/10.1016/j.culher.2023.06.020>.

26. Turk N, Dearman WR. Assessment of grouting efficiency in a rock mass in terms of seismic velocities. *B Eng Geol Environ*. 1987;36:101–8. <https://doi.org/10.1007/BF02600944>.
27. De Araújo MT, Silva JH, Aquino Rocha EC, Barreto Monteiro YV, Póvoas ER, Kohlman Rabbani. Evaluation of the ultrasound test for estimating the depth of cracks in concrete. *Revista de La Asociación Latinoamericana de Control de Calidad, Patología y Recuperación de La Construcción*. 2018;9:79–92. <https://doi.org/10.21041/ra.v9i1.289>.
28. Bungey JH, Millard SG, Grantham MG, Millard SG, Grantham MG. *Testing of concrete in structures*. 4th ed. London: Taylor & Francis; 2006.
29. BS 1881. Part 203, Recommendations for measurement of the velocity of ultrasonic pulses in concrete, London, 1986.
30. Medeiros A, Padaratz LJ, Pinto RCA, Andrade PB. Use of ultrasound to estimate depth of surface opening cracks in concrete structures. *eJNDT*. 2010;8:1–11.
31. Zhang J, Chen W, Li Z, Wang X, Guo Q, Wang N. Study on workability and durability of calcined ginger nuts-based grouts used in anchoring conservation of earthen sites. *J Cult Herit*. 2015;16:831–7. <https://doi.org/10.1016/j.culher.2015.02.007>.
32. Zhou J, Wang X, Pei Q, Liu H, Li Z, Yu J. Effect of the pulping process on mechanical properties of slurry stones. *J Lanzhou University: Nat Sci*. 2020;56:125–32. <https://doi.org/10.13885/j.issn.0455-2059.2020.01.016>.
33. Li J, Zhang X, Xiao L, Liu K, Li Y, Zhang Z, Chen Q, Ao X, Liao D, Gu Y, Ma M, Yu X, Xiang Q, Chen J, Zhang X, Yang T, Penttinen P, Zhao K. Changes in soil microbial communities at Jinsha earthen site are associated with earthen site deterioration. *BMC Microbiol*. 2020;20:147. <https://doi.org/10.1186/s12866-020-01836-1>.
34. Richards J, Zhao G, Zhang H, Viles H. A controlled field experiment to investigate the deterioration of earthen heritage by wind and rain. *Herit Sci*. 2019;7:51. <https://doi.org/10.1186/s40494-019-0293-7>.
35. Li W, Zhang J, W N, Shi Z, An C, Yan F. Application of non-destructive testing to evaluate the grouting reinforcement effect of fissures in earthen sites. *J Lanzhou University: Nat Sci*. 2023;59(1):80–9. <https://doi.org/10.13885/j.issn.0455-2059.2023.01.011>.
36. Zhang N, Liu X, Lan H. Characterizing saturation state of loess using P-wave velocity. *Eng Geol*. 2021;290:106207. <https://doi.org/10.1016/j.enggeo.2021.106207>.

Publisher's Note

Springer Nature remains neutral with regard to jurisdictional claims in published maps and institutional affiliations.